
Chapter 6
Cell line studies

CHAPTER-6 CYTOTOXICITY AND CELLULAR UPTAKE STUDIES

6.1 Introduction

Cancer-selective delivery systems are highly desired for chemotherapeutic agents for their ability to efficiently deliver the drug to the cancer cells. By confining the cytotoxic activity of the anticancer drugs to within the malignant tissues, such delivery systems are envisaged to minimize indiscriminate drug distribution and lead to a focused destruction of the cancerous cells. The aim of the present study was therefore to evaluate the cytotoxicity of the formulated PLGA nanoparticles of the two drugs etoposide and Cytarabine and also study their cellular uptake in the two cancer cell lines, L1210 and DU145.

Cytotoxicity studies were carried out on L1210 and DU145 cells for 1,3 and 5 days using the 3-(4,5- dimethylthiazol-2-yl)-2,5-diphenyltetrazolium bromide (MTT) assay (Cole, 1986). Yellow MTT (3-(4,5-Dimethylthiazol-2-yl)-2,5- diphenyltetrazolium bromide, a tetrazole) is reduced to purple formazan in the mitochondria of living cells. The absorbance of this colored solution can be quantified by measuring at a certain wavelength (usually between 500 and 600 nm) by a spectrophotometer (Freshney, 1994). The absorption is dependent on the solvent employed. This reduction takes place only when mitochondrial reductase enzymes are active, and therefore conversion can be directly related to the number of viable (living) cells. When the amount of purple formazan produced by cells treated with an agent is compared with the amount of formazan produced by untreated control cells, the effectiveness of the agent in causing death of cells can be deduced, through the production of a dose-response curve. The resulting purple solution is spectrophotometrically measured. An increase in cell number results in an increase in the amount of MTT formazan formed and an increase in absorbance.

6.2 Materials

Table 6.1 gives the list of materials and their sources.

Table 6.1
List of materials

Material	Source
Etoposide, Cytarabine	Gift sample from Biocon, Bangalore
PLGA	Gift sample from Boehringer Ingelheim Limited, Germany.
Pluronic F-68 (BASF)	Gift sample from Alembic Ltd, Vadodara
Chloroform AR grade	SD Fine Chemicals, Mumbai
Methanol AR grade	SD Fine Chemicals, Mumbai
Acetone AR grade	SD Fine Chemicals, Mumbai
6- Coumarin	Polysciences Inc., USA
3-(4,5-dimethylthiazol-2-yl)-2,5-diphenyltetrazolium bromide (MTT) (Sigma, St. Louis, USA)	Gift sample from NIRRH, Mumbai
L1210 cell line	National Center for Cell Sciences, Pune
DU 145 cell line	National Center for Cell Sciences, Pune
Dulbecco's Modified Eagle Medium (DMEM), supplemented with 100 U/mL penicillin and 100 µg/mL streptomycin with 10% fetal bovine serum (Sigma, USA)	Gift sample from NIRRH, Mumbai
Fluoromount-G	Southern Biotech Associates, USA
Glacial acetic acid	S.D.Fine Chemicals, Mumbai
Potassium dihydrogen phosphate	S.D.Fine Chemicals, Mumbai
Disodium hydrogen phosphate	S.D.Fine Chemicals, Mumbai
Potassium chloride	S.D.Fine Chemicals, Mumbai
Sodium chloride	S.D.Fine Chemicals, Mumbai
Sodium hydroxide.	S.D.Fine Chemicals, Mumbai
Polycarbonate membrane 0.2, 0.45 and 2 µm 25mm	Whatman, USA

6.3 Maintenance and subculturing of Cell lines

L1210 mouse leukaemia cell line was obtained from National Center for Cell Sciences, Pune and was maintained in DMEM media supplemented with 100 U/mL penicillin and 100 µg/mL streptomycin with 10% fetal bovine serum at 37°C in a 5% CO₂ humidified atmosphere. L1210 was grown as a suspension culture.

DU 145 cells were obtained from National Center for Cell Sciences, Pune and were maintained in DMEM media supplemented with 100 U/mL penicillin and 100 µg/mL streptomycin with 10% fetal bovine serum at 37°C in a 5% CO₂ humidified atmosphere. DU 145 cells were grown as monolayer culture.

SECTION A-CYTOTOXICITY STUDIES

6.4 Cytotoxicity assay

Cytotoxicity was determined by the use of 3-(4,5-dimethylthiazol-2-yl)-2,5-diphenyltetrazolium bromide (MTT) assay (Cole, 1986). Briefly, 100 μ l of L1210 or DU145 cell (5×10^4 cells/mL) were seeded onto each well of 96-well plate (Corning Incorporated Life Sciences, Acton, MA, USA) and incubated for 24 h at 37°C in a humidified CO₂ atmosphere. After incubation, 100 μ L of DMSO medium containing test sample (pure drug, Blank NP or drug loaded NP at a concentration of 5, 10, 20, 50 and 100 μ M) or complete medium for untreated controls were distributed in the 96-well plates and plates were then incubated at 37°C for 24 h. The culture medium was subsequently removed and medium containing 20 μ l MTT reagent (5 mg/mL) was added to each culture well. After 4 h of incubation, the cells were washed carefully with PBS and the crystals were dissolved by the addition of 10% SDS for 20 min with occasional shaking. Finally, absorbance, at λ_{570} test wavelength and λ_{630} reference wavelength, was measured using an automated microplate reader (Labsystem Multiskan, Helsinki, Finland). In each experiment, the test sample was analyzed in six individual wells. Cell survival was estimated as a percentage of the corresponding control.

IC₅₀ determination

The concentration of drug or NP formulation required to inhibit cell proliferation by 50% (IC₅₀) was determined by plotting the percentage of cell growth inhibition versus the concentration of pure drug or NP formulation.

Statistical analysis

All values were expressed as mean \pm SD. The data were statistically analyzed by one-way ANOVA. P values <0.05 were considered significant.

6.5 Results and discussions of cytotoxicity studies of etoposide and etoposide loaded PLGA nanoparticles

Cell cytotoxicities of ETO, ETO-PLGA NP, ETO-PLGA-MPEG NP and ETO-PLGA-PLU NP for L1210 and DU145 cells were investigated. The % viability obtained for L1210 cells as shown in Table 6.2 and Fig. 6.1 reveal that ETO showed lower cytotoxicity compared to its nanoparticulate formulations. PLGA based NP formulations played an important role in enhancing the cytotoxic effect of ETO, which was probably due to increase in their intracellular uptake. MTT assay on L1210 viability showed that the cytotoxicity of ETO and ETO loaded NP was concentration depended and there was decrease in the viability of the L1210 cells as the concentration was increased from 5 to 100 μM . Concentrations above 100 μM were not tested as the values of IC_{50} were determinable within the range tested.

The IC_{50} values for L1210 cells were 18.0, 6.2, 4.8 and 5.4 μM for ETO, ETO-PLGA NP, ETO-PLGA-MPEG NP and ETO-PLGA-PLU NP respectively. The IC_{50} values significantly decreased ($p > 0.005$) in the nanoparticulate formulations than the free drug (Fig. 6.3a). The IC_{50} values decreased 2.9 times for ETO-PLGA NP, 3.7 and 3.3 times for ETO-PLGA-MPEG NP and ETO-PLGA-PLU NP respectively compared with free drug. The order of cytotoxicity was ETO-PLGA-PLU NP > ETO-PLGA-MPEG NP > ETO-PLGA NP > ETO.

Similarly in DU145 cells, the cytotoxicity of the drug loaded NP was more than the free drug ETO. Table 6.3 and Fig. 6.2 show % Viability of DU145 cells by MTT Assay using Plain drug etoposide (ETO), and Etoposide loaded NPs ETO-PLGA NP, ETO-PLGA-MPEG NP and ETO-PLGA-PLU NP. The IC_{50} values for DU145 cells were 98.4, 75.1, 60.1 and 71.3 μM for ETO, ETO-PLGA NP, ETO-PLGA-MPEG NP and ETO-PLGA-PLU NP respectively as shown in Fig. 6.3b. The IC_{50} values significantly decreased ($p > 0.005$) in the nanoparticulate formulations than the free drug. The IC_{50} values decreased 1.3 times for ETO-PLGA NP, 1.6 and 1.4 times for ETO-PLGA-MPEG NP and ETO-PLGA-PLU NP respectively compared with free drug. The order of cytotoxicity was ETO-PLGA-MPEG NP > ETO-PLGA-PLU NP > ETO-PLGA NP > ETO.

It was seen that the IC_{50} values of pure drug etoposide was decreased when it was loaded in NPs. The results are in comparison to study by Patlolla and Venkateswarlu (2008), which showed that the IC_{50} value of the pure drug etoposide was decreased when it was encapsulated in lipid nanosphere. They found that on KB cell line, IC_{50} values of etoposide pure drug solution was 33 μ M, whereas it was decreased to 5 μ M in the nanosphere form.

Comparing the results of the cytotoxicity studies of ETO for the two cell lines, L1210 and DU145, it was seen that both ETO and ETO loaded NP had lower IC_{50} values for L1210 cells. Hence lower doses of ETO or ETO loaded NP would be required in the therapy of leukaemia than in prostate cancer. The study indicates the probable reason why etoposide is generally recommended for treating leukaemia rather than prostate cancer.

It was concluded from the cytotoxicity studies that the nanoparticulate formulations of ETO had lower IC_{50} values than the pure drug and among the three NP formulations; Eto-PLGA-Pluronic NP had the highest cytotoxicity effect on L1210 and ETO-PLGA-MPEG NP on DU145 cells.

Table 6.2
In-vitro cytotoxicity of Etoposide and Etoposide loaded NP on L1210 cells (% Viability \pm SD) by MTT Assay

Concentration (μ M)	% Viability (\pm SD)			
	Etoposide	Eto-PLGA NP	Eto-PLGA-MPEG NP	Eto-PLGA-Pluronic NP
0	100 \pm 0.0	100 \pm 0.0	100 \pm 0.0	100 \pm 0.0
5	68.5 \pm 2.1	55.5 \pm 1.1	48.7 \pm 1.4	52.2 \pm 0.4
10	58.4 \pm 1.1	44.2 \pm 2.1	47.8 \pm 1.1	47.3 \pm 2.1
20	48.2 \pm 0.8	40.3 \pm 3.0	45.4 \pm 2.2	41.4 \pm 1.1
50	45.1 \pm 1.0	38.1 \pm 0.1	41.9 \pm 0.2	36.2 \pm 2.1
100	40.0 \pm 1.1	35.0 \pm 1.2	39.1 \pm 0.7	31.1 \pm 0.2

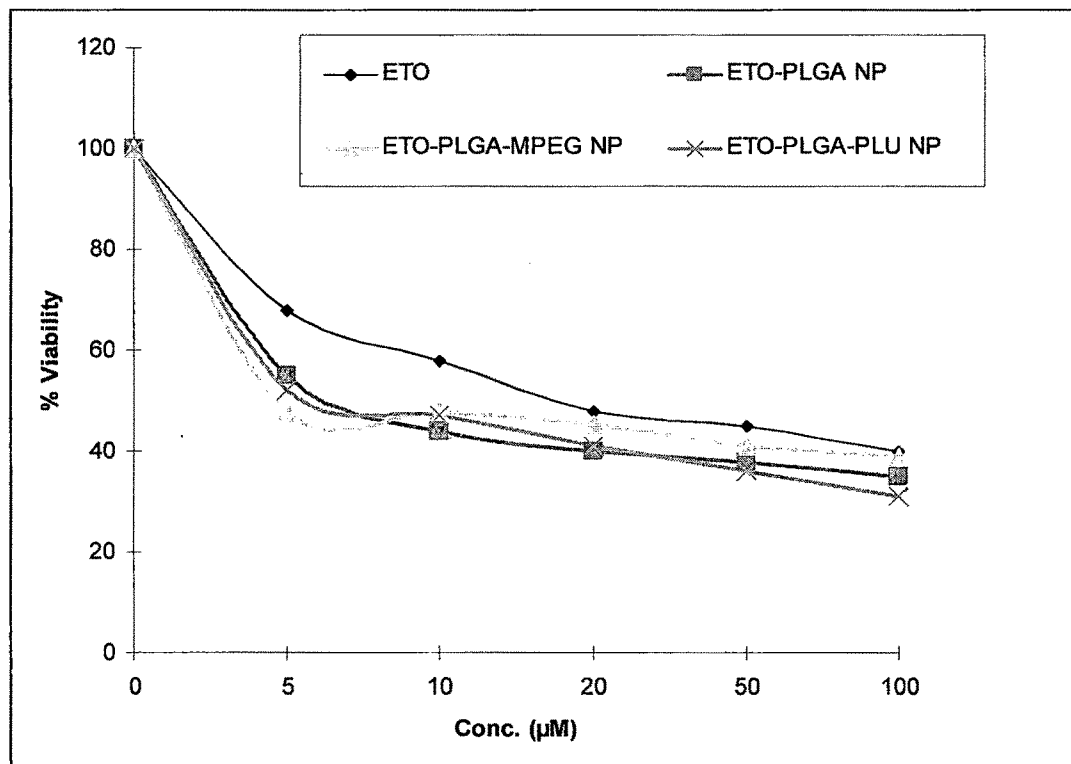


Fig. 6.1: % Viability of L1210 cells by MTT Assay using Plain drug etoposide (ETO), and Etoposide loaded NPs ETO-PLGA NP, ETO-PLGA-MPEG NP and ETO-PLGA-PLU NP.

Table 6.3
In-vitro cytotoxicity of Etoposide and Etoposide loaded NP on DU 145 cells (% Viability \pm SD) by MTT Assay

Concentration (μ M)	% Viability (\pm SD)			
	Etoposide	Eto-PLGA NP	Eto-PLGA-MPEG NP	Eto-PLGA-Pluronic NP
0	100 \pm 0.0	100 \pm 0.0	100 \pm 0.0	100 \pm 0.0
5	86.4 \pm 3.1	74.3 \pm 1.1	66.8 \pm 1.0	71.8 \pm 1.0
10	81.2 \pm 1.1	68.4 \pm 0.3	58.0 \pm 1.8	66.0 \pm 1.8
20	85.5 \pm 1.4	61.2 \pm 0.6	54.1 \pm 1.4	59.1 \pm 1.4
50	55.2 \pm 1.3	55.7 \pm 1.3	50.4 \pm 1.2	52.4 \pm 0.2
100	49.5 \pm 2.1	44.4 \pm 1.8	41.2 \pm 1.3	46.2 \pm 1.3

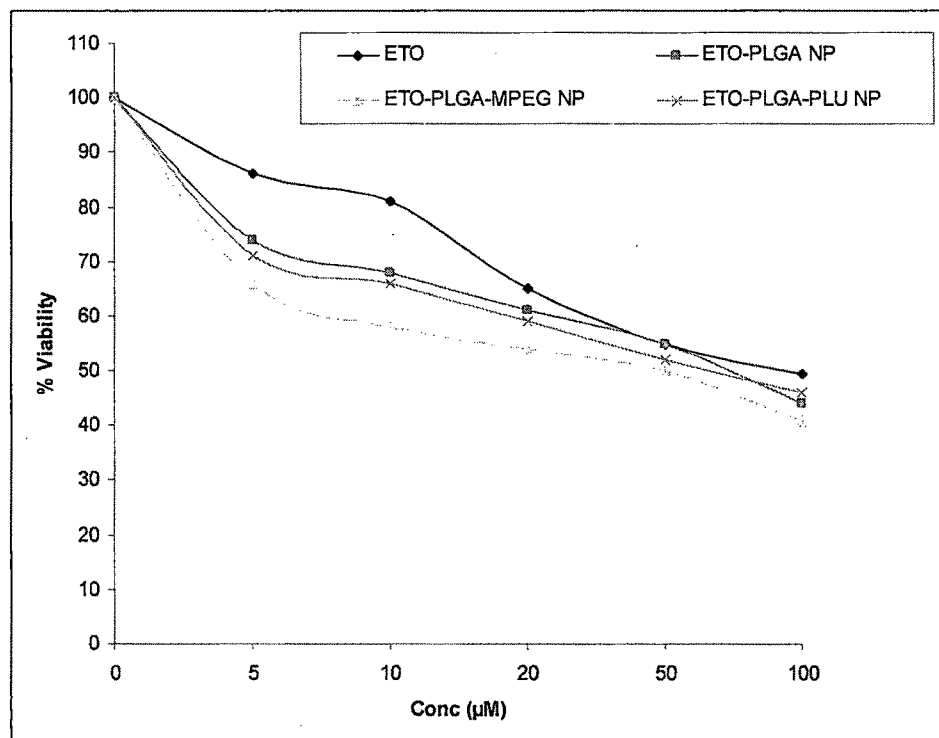


Fig. 6.2: % Viability of DU145 cells by MTT Assay using Plain drug etoposide (ETO), and Etoposide loaded NPs ETO-PLGA NP, ETO-PLGA-MPEG NP and ETO-PLGA-PLU NP.

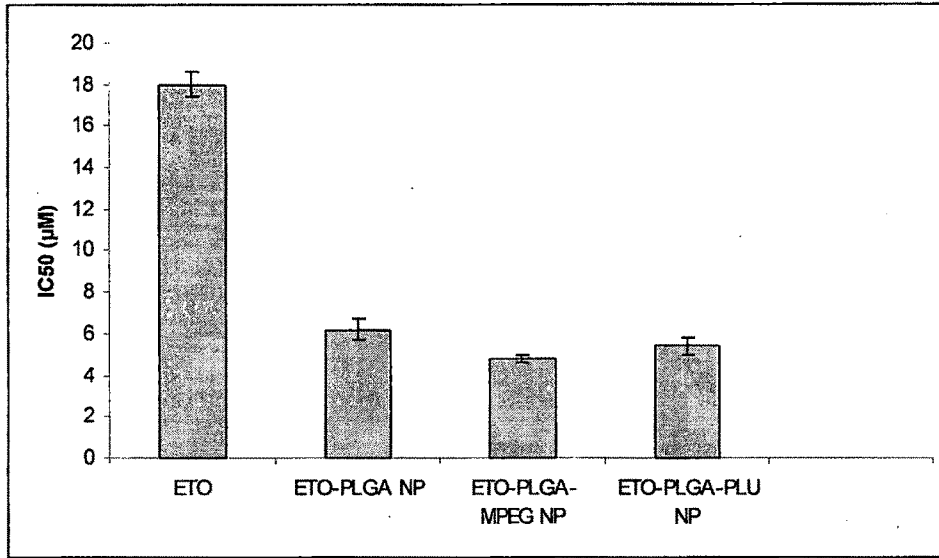


Fig 6.3a: IC₅₀ values of ETO, ETO-PLGA NP, ETO-PLGA-MPEG NP and ETO-PLGA-PLU NP for L1210 cells

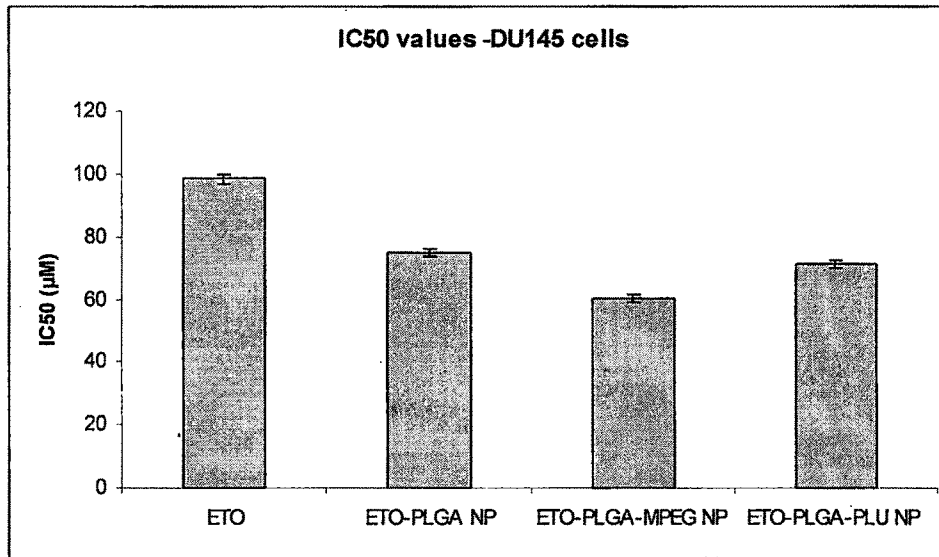


Fig 6.3b: IC₅₀ values of ETO, ETO-PLGA NP, ETO-PLGA-MPEG NP and ETO-PLGA-PLU NP for DU145 cells

6.5.1 Long term cytotoxicity study

A relatively short incubation period used in the MTT-based cytotoxicity assay (24 or 48 h) is not enough to determine long-term cytotoxicity of the nanoparticulate formulations, and a more prolonged incubation time would be required to fully exert the cytotoxicity effect of nanoparticles (Yoo and Park, 2004). Moreover, after the nanoparticles reach the cytoplasm they must be solubilized in a molecularly dissolved state prior to reaching the nucleus to exert cytotoxic effect. Zhang and Feng (2006) studied cancer cell viability by MTT assay of paclitaxel -loaded PLA-TPGS nanoparticles on day 1, 2 and 3 and found that on 3rd day, the IC₅₀ values were significantly reduced. Hence, in the present study time based cytotoxicity on L1210 cell lines were carried out for 1, 3 and 5 days.

Table 6.4 shows time based cytotoxicity study of ETO and ETO loaded NP on L1210 cells by MTT Assay.

Table 6.4
Time based Cytotoxicity study on L1210 cells by MTT Assay

Sr. No.	Formulation	IC ₅₀ μ M \pm SD		
		Day1 (24h)	Day3 (72h)	Day 5 (120h)
1	ETO	18.0 \pm 0.6	17.6 \pm 0.4	17.3 \pm 0.3
2	ETO-PLGA NP	6.2 \pm 0.5	4.1 \pm 0.5	3.4 \pm 0.5
3	ETO-MPEG-PLGA NP	5.4 \pm 0.4	3.5 \pm 0.4	2.2 \pm 0.3
4	ETO-PLGA-PLU NP	4.8 \pm 0.2	3.3 \pm 0.2	2.4 \pm 0.2

The study showed that the cytotoxicity of ETO pure drug solution on L1210 cells did not have any significant change in the IC₅₀ values on the 3rd and 5th day. But the IC₅₀ values significantly decreased on 3rd and 5th day for all the three nanoparticulate formulations. This was probably due to the fact that pure drug solution exerted its maximum cytotoxic effect within 24 hours and hence there was no further significant decrease in the viability of the L1210 cells on the 3rd and 5th day.

The three NP formulations had a significant decrease in the viability of the L1210 cells on the 3rd and 5th day. The nanoparticles showed their cytotoxic effect once the drug was released from the NPs and solubilized either in the cytoplasm or in the nucleus. Among the three NP formulations, ETO-MPEG-PLGA NP had a comparatively lower IC₅₀ value on the 5th day, indicating its better efficiency in inhibiting cells for a sustained period. The results are in accordance with our in-vitro drug release studies, where the drug from ETO-MPEG-PLGA NP was sustained for a period of 7 days.

The study concluded that the drug loaded PLGA nanoparticulate formulations were efficient in decreasing the viability of the L1210 cells over a period of three days, whereas the pure drug exerted its maximum efficiency on the day one itself.

6.5.2 Cytotoxicity study of the polymers used

The three different polymers PLGA, PLGA-MPEG and PLGA-PLURONIC used in the NP formulations were also tested for their cytotoxicities at two concentrations, AC (actual concentration used in the NP formulation) and DC (double concentration used in the NP formulation). The polymers were dissolved in DMSO and then filtered by 0.22 μ filter before carrying out the MTT assay as explained in section 6.4.

Table 6.5 gives % Viability values for PLGA, PLGA-MPEG and PLGA-PLURONIC polymers on L1210 cells and DU145 cells after 48h. It was seen that viability was more than 99% in AC and DC for PLGA and more than 97% for PLGA-MPEG and PLGA-PLURONIC. This confirmed that the used polymers did not have their own cytotoxicity effect on the cells in the concentrations used.

Table 6.5
Cytotoxicity study of polymers on L1210 cells and DU145 cells by MTT Assay

Formulation	Concentration	% Viability	% Viability
		(\pm SD) L1210 cell line	(\pm SD) DU145 cells
PLGA	AC	99.4 \pm 0.12	99.5 \pm 0.17
	DC	99.2 \pm 0.10	99.1 \pm 0.12
PLGA-Pluronic	AC	97.8 \pm 0.12	97.7 \pm 0.21
	DC	97.1 \pm 0.20	97.1 \pm 0.19
PLGA-mPEG	AC	99.1 \pm 0.06	99.4 \pm 0.09
	DC	98.2 \pm 0.18	98.9 \pm 0.20

The study concluded that the cytotoxicity was observed for the drug loaded NP on L1210 and DU145 cells was due to the release of the entrapped drug from the NP and not because of the polymers used.

6.6 Results and Discussions: cytotoxicity studies on cytarabine and cytarabine Loaded PLGA Nanoparticles

Cytotoxicity of CYT, CYT -PLGA NP and CYT -PLGA-MPEG NP were studied on two cell lines, L1210 and DU145. The percent viability of L1210 cells after treatment with CYT, CYT -PLGA NP and CYT -PLGA-MPEG NP are shown in Table 6.6 and Fig. 6.4. The study shows that pure drug CYT showed lower cytotoxicity compared to its nanoparticulate formulations. The increase in cytotoxicity may be attributed to increase in the intracellular uptake of the NPs than the free drug (Panyam et al., 2004). Fig. 6.4 demonstrates that the viability of the L1210 cells was decreased as the concentration of the drug was increased and hence the viability is said to be concentration dependent. The IC_{50} values for L1210 cells were 6.5, 5.3, and 2.2 μ M for CYT, CYT -PLGA NP and CYT -PLGA-MPEG NP respectively (Fig.6.6a). IC_{50} values significantly decreased in the nanoparticulate formulations than the free drug. The IC_{50} values decreased 1.2 times for CYT-PLGA NP and 2.9 times for CYT-PLGA-MPEG NP compared with free drug. The order of cytotoxicity was CYT-PLGA-MPEG NP > CYT-PLGA NP >CYT.

Similarly in DU145 cells, the cytotoxicity of the drug loaded NP was more than the free drug CYT. Table 6.7 and Fig. 6.5 show the in-vitro cytotoxicity of Cytarabine and Cytarabine loaded NP on DU 145 cells by the MTT assay. It was seen that as the concentration of the drug was increased, the % viability of DU145 cells was decreased. The IC_{50} values for DU145 cells were 62.5, 20.2, and 14.3 μ M respectively for CYT, CYT -PLGA NP and CYT -PLGA-MPEG NP respectively as shown in Fig.6.6b. The cytotoxicity studies found that IC_{50} values significantly decreased in the nanoparticulate formulations than the free drug. The IC_{50} values decreased 3.0 times for CYT-PLGA NP and 4.3 times for CYT-PLGA-MPEG NP compared with free drug. The order of cytotoxicity was CYT-PLGA-MPEG NP > CYT-PLGA NP >CYT.

Comparing the results of the two cell lines, it was seen that CYT was having lower IC_{50} for L1210 cells (leukaemic cells) than the DU145 cells (prostate cancer cells) as expected because CYT is mostly recommended in leukaemia therapy rather than treatment of prostate cancer.

Table 6.6
In-vitro cytotoxicity of Cytarabine and Cytarabine loaded NP on L1210 cells (% Viability \pm SD) by MTT Assay

Concentration (μ M)	% Viability (\pm SD)		
	Cytarabine	CYT-PLGA NP	CYT-PLGA-MPEG NP
0	100 \pm 0.0	100 \pm 0.0	100 \pm 0.0
5	59.3 \pm 3.7	52 \pm 1.1	52.7 \pm 1.4
10	43.4 \pm 1.4	42 \pm 1.0	44.8 \pm 1.1
20	32.1 \pm 3.3	30 \pm 1.4	41.4 \pm 2.2
50	31.3 \pm 1.2	28 \pm 2.0	30.9 \pm 0.2
100	28.2 \pm 2.1	27 \pm 1.1	25.1 \pm 0.7

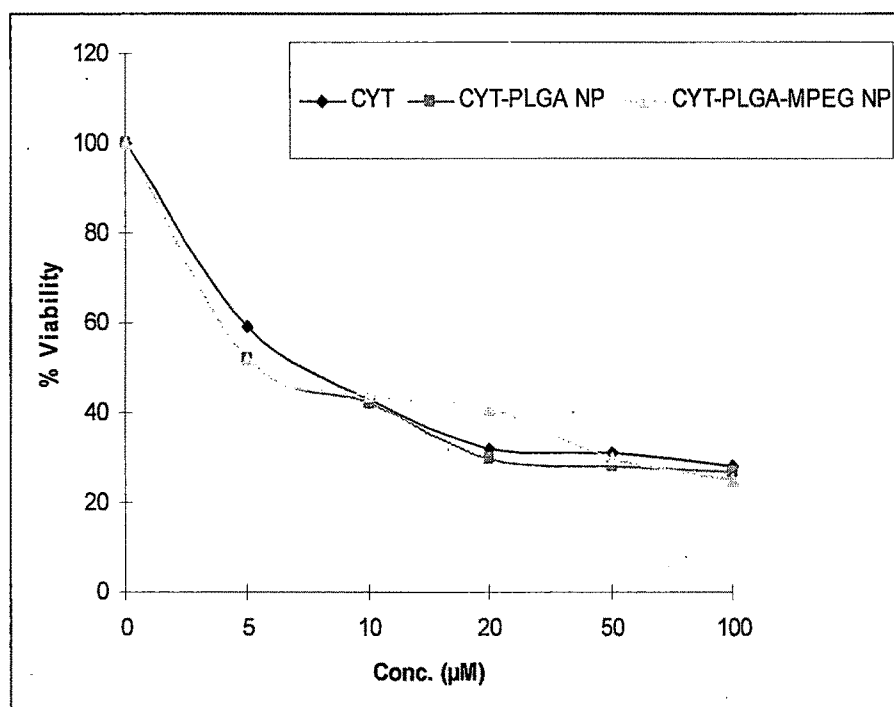


Fig. 6.4: % Viability of L1210 cells by MTT Assay using Plain drug Cytarabine and (CYT), and Cytarabine loaded NPs CYT-PLGA NP, CYT-PLGA-MPEG NP.

Table 6.7
In-vitro cytotoxicity of Cytarabine and Cytarabine loaded NP on DU 145 cells (% Viability \pm SD) by MTT Assay

Concentration (μ M)	% Viability (\pm SD)		
	Cytarabine	CYT-PLGA NP	CYT-PLGA-MPEG NP
0	100 \pm 0.0	100 \pm 0.0	100 \pm 0.0
5	73.5 \pm 2.1	63.3 \pm 1.1	58.6 \pm 2.0
10	63.3 \pm 1.3	53.2 \pm 2.2	51.9 \pm 1.1
20	55.2 \pm 3.4	50.5 \pm 0.1	47.2 \pm 1.2
50	51.5 \pm 1.5	48.2 \pm 1.1	41.1 \pm 1.2
100	44.7 \pm 2.2	41.8 \pm 0.3	37.4 \pm 1.3

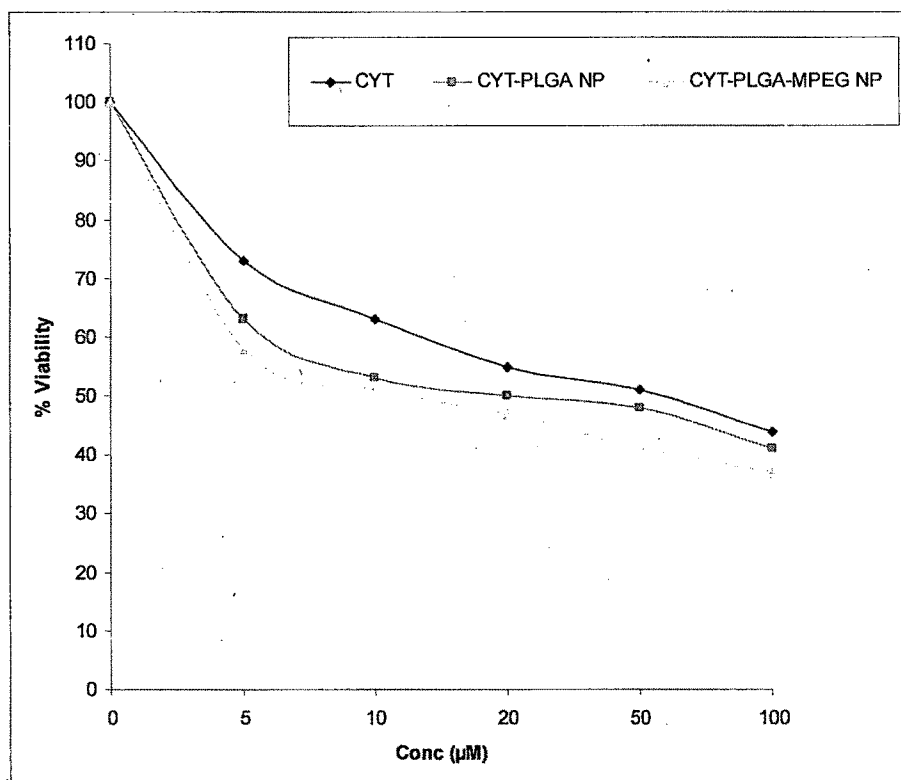


Fig. 6.5: % Viability of DU145 cells by MTT Assay using Plain drug Cytarabine and (CYT), and Cytarabine loaded NPs CYT-PLGA NP, CYT-PLGA-MPEG NP.

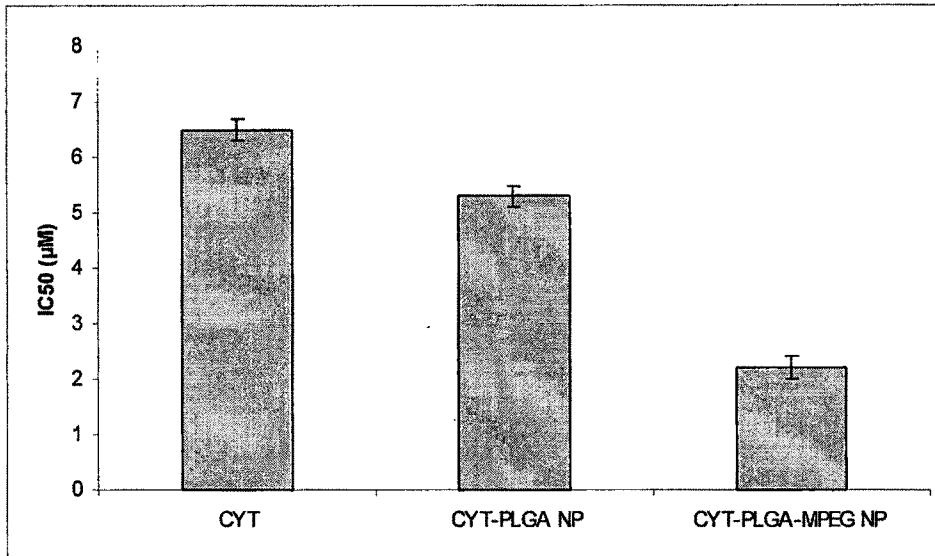


Fig 6.6a: IC50 values of CYT, CYT-PLGA NP, CYT-PLGA-MPEG NP for L1210 cells

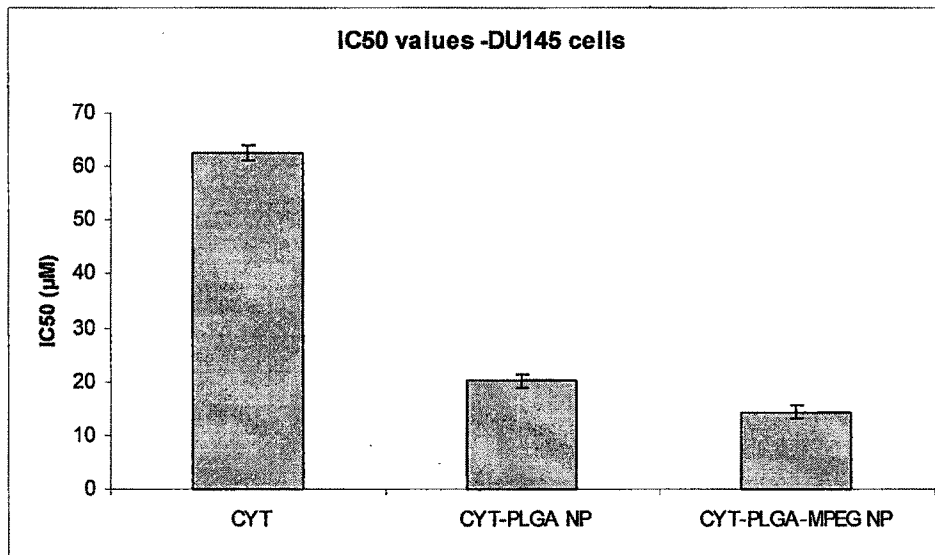


Fig 6.6b: IC50 values of CYT, CYT-PLGA NP, CYT-PLGA-MPEG NP for DU145 cells

Long term cytotoxicity study

Table 6.8 shows IC₅₀ values for time based cytotoxicity study of CYT, CYT-PLGA NP and CYT-MPEG NP on L1210 cells by MTT Assay on 1, 3 and 5 days. It was seen that there was no significant change in the IC₅₀ values of pure drug solution (CYT) on the 3rd and 5th day. A significant difference was observed in the IC₅₀ values in both CYT-PLGA NP and CYT-MPEG-PLGA NP. The decreasing pattern of IC₅₀ value with respect to time was similar for both the nanoparticulate formulations. The IC₅₀ value of CYT-PLGA NP reduced from initial 5.3 to 4.1 and 2.7 μ M and CYT-PLGA-PEO NP reduced from initial IC₅₀ value of 2.2 to 1.8 and 0.8 μ M in 3 and 5 days respectively. Maximum reduction of 2.5 times of the initial IC₅₀ value was seen in CYT-MPEG-PLGA NP on the 5th day.

Table 6.8
Time based Cytotoxicity study of CYT, CYT-PLGA NP and CYT-MPEG NP on L1210 cells by MTT Assay

Sr. No.	Formulation	IC ₅₀ Day1 μ M \pm SD	IC ₅₀ Day3 μ M \pm SD	IC ₅₀ Day 5 μ M \pm SD
1	CYT	6.5 \pm 0.6	6.0 \pm 0.4	5.8 \pm 0.3
2	CYT-PLGA NP	5.3 \pm 0.5	4.1 \pm 0.5	2.7 \pm 0.5
3	CYT-MPEG-PLGA NP	2.2 \pm 0.2	1.8 \pm 0.1	0.8 \pm 0.1

The results of the cytotoxicity studies indicate that the pure drug CYT was completely utilized on the day 1 and did not show any significant effect on the consecutive days, indicating that CYT showed its maximum efficiency on the day 1. Comparatively the nanoparticles, released the entrapped drug for a longer duration and showed a significant change in the IC₅₀ values upto 5 days. Hence it was concluded that CYT loaded nanoparticles had long term cytotoxic affect on the L1210 cells.

SECTION B- CELLULAR UPTAKE STUDIES

6.7 Introduction

Intracellular delivery of the therapeutic agents refers to the delivery of the drug within the cell. Intracellular delivery potentiates the pharmacologic effect of the drug. Therapeutic efficiency of anticancer drugs is improved if they are delivered intracellularly in the cells (Panyam et al., 2004). Cellular uptake studies of polymeric nanoparticles demonstrate the therapeutic effects of the drug-loaded NPs at the cellular level (Win and Feng, 2005; Dong and Feng, 2004). The cellular uptake of the drug-loaded NPs would depend on internalization and retention of the NPs by the diseased cells. Even though in-vivo and in-vitro biological process could be very much different, but in-vitro cell line investigation provides preliminary evidence of the therapeutic effects of the NPs over the free drug. It has been reported that NPs have higher cell uptake efficiency compared with that of free drug (Lin et al., 2005).

Confocal microscopy has been widely used to localize and to quantify the uptake of particles by the cancer cells. Confocal microscopy offers the main advantage of giving a three-dimensional view of the samples. Furthermore, sample preparation is easier and this technique gives information on particle penetration in the tissue layer (Pawley, 1995). Confocal microscopy has proved valuable, being used frequently in the study of nanoparticle uptake in biological tissues such as eye (de Campos et al., 2004), brain (Ramge et al, 2000), and skin (Shim et al., 2004). Confocal laser scanning microscopy demonstrated an effective internalization of the nanoparticles by HER2-overexpressing cells via receptor-mediated endocytosis (Wartlick et al., 2004). Confocal microscopy gives information on the fate of a nanoparticle containing fluorescent dyes or drugs (Yoo and Park, 2004).

6-coumarin, a fluorescent marker, is reported to be a useful probe for marking the PLGA nanoparticles in the cellular uptake study. 6-coumarin has a low dye loading, low leakage rate, biocompatibility and high fluorescence activity (Young et al., 1991). Moreover, the uptake of 6-coumarin does not cause significant changes in the morphology of the nanoparticles. The cellular uptake of the PLGA nanoparticles containing 6-coumarin can be quantified by measuring the fluorescence intensity of the

nanoparticles and they can be visualized by use of confocal laser scanning microscopy (CLSM).

6.8 Preparation of 6-coumarin loaded nanoparticles

To investigate the in vitro cellular uptake of NP, fluorescent NPs were prepared by substituting drug with 6- coumarin (0.01 % w/w), using solvent evaporation technique. A solution of 6-coumarin and PLGA in chloroform was emulsified into distilled water containing Pluronic F-68 (0.1%w/v). This primary emulsion was passed through high pressure homogenizer (Emulsiflex, C5, Avestin, Canada) for 4 cycles at 10000 psi pressure. The homogenized O/W emulsion was immediately added drop-wise to an aqueous solution of Pluronic F-68 and the contents were stirred overnight with a magnetic stirrer (Remi Equipments, Mumbai) to evaporate the chloroform. Nanoparticles were recovered by centrifugation for 30 min at 25000 rpm, washed and lyophilized (Heto Dry Winner, Denmark) for 24 hrs to yield freeze dried nanoparticles. Samples were frozen at -70°C and placed immediately in the freeze-drying chamber. 6-coumarin loaded PLGA-MPEG NP and PLGA-PLURONIC NP were prepared similarly.

6.9 Cell uptake efficiency

L1210 cells were plated in Falcon 96-well black plates at a density of 5×10^3 cells/well and after the cells reached 80% confluence (cells were counted by hemacytometer using Light microscope) the culture medium (DMEM supplemented with 100 U/mL penicillin and 100 $\mu\text{g}/\text{mL}$ streptomycin with 10% fetal bovine serum) was changed with that containing 6-coumarin loaded NPs. The particles were dispersed in the DMSO medium at concentration of 50, 100, 200 and 250 mg/ml for 2 h. After incubation, the suspension was removed and the wells were washed three times with 50 ml of PBS to eliminate traces of NPs left in the wells. After that, 50 ml of 0.5% Triton X-100 in 0.2 N NaOH was added to the sample wells to lyse the cells. The amount of fluorescence present in each well was then measured by microplate reader with excitation wavelength at 430nm and emission wavelength at 485nm. The fluorescent intensity was used for quantitative study of the uptake as explained by Win et al. (2005). Results obtained were expressed as a percentage of the total intensity of fluorescent labeled nanoparticles found in the solubilized cells to the total intensity of fluorescent labeled nanoparticles in the cells.

6.10 Confocal microscopy

Confocal microscopy was used to visualize cellular uptake of the nanoparticles by cells as described by Yoo and Park (2004). After initial passage in tissue culture flasks, cells were grown to semi-confluence in DMEM supplemented media in 6-well tissue culture plates on Corning's circular glass cover-slips at 37°C and 5% CO₂ atmosphere. After filtration, the nanoparticle suspension was incubated with the cells at 37°C for a period of 1, 2, 3, 4 and 24 h. The media was then removed and the plates were washed thrice with sterile PBS. After the final wash, the cells were fixed with 4% (v/v) paraformaldehyde in PBS for 1.0 h at room temperature and were washed four times with PBS. Individual cover-slips were then mounted cell side up on clean glass slides with fluorescence-free glycerol based mounting medium Fluoromount-G. Differential interference contrast (DIC) and fluorescence images were acquired with a confocal microscope (Zeiss Confocal LSM 410, USA) at an excitation wavelength of 495nm and an emitting wavelength of 520 nm. Z-stack Images were also taken to give a visual presentation of the NP uptake in each section of the cell at different cell depths.

6.11 Flow Cytometry

For flow cytometry analysis, cells were incubated with nanoparticles (6 coumarin was used as fluorescent marker) in DMEM supplemented with 10% fetal bovine serum (FBS). After 4 h of incubation, the cells were washed with PBS and then harvested for further analysis. The cells (1×10^4 counts) were analyzed by flow cytometry (FACS Calibur, USA) with a forward scattering (FSC) range between 200 and 600 in a linear scale (Yoo and Park, 2004).

6.12 Statistical Methods

All data were processed and analyzed by Sigma-Plot 8.0 software (SPSS, IL). The statistical significances were evaluated by t-test of the software and p value less than 0.05 was accepted as statistically significant.

6.13 Results and Discussion

6.13.1 Cellular uptake efficiency

The time and concentration dependent cellular uptake of the NPs was determined by quantifying the percentage of fluorescence. The uptake of fluorescent NPs by DU145 cells over an interval of 0.5, 1, 2 and 4h is shown in Fig. 6.7. It was seen that the uptake of the NPs was increased with time from 28 to 38% for PLGA NP, 32 to 47 for PLGA-MPEG NPs and 33 to 50% for PLGA-PLURONIC NPs in 30 min to 4h respectively. Fig 6.8 shows concentration dependent uptake for NPs in DU145. Uptake of PLGA NP increased to 38% for 100 $\mu\text{g/ml}$ but was reduced with further increase in concentration. Similarly, there was a reduction in the uptake of PLGA-MPEG NP and PLGA-PLURONIC NP at higher concentration of 200 $\mu\text{g/ml}$ and 250 $\mu\text{g/ml}$. Highest uptake of 47% and 50% was achieved at 100 $\mu\text{g/ml}$ concentration for PLGA-MPEG NP and PLGA-PLURONIC NP respectively.

Similarly for L1210 cells (Fig. 6.9), the uptake increased from 15 to 50% for PLGA NP, from 23 to 65 for PLGA-MPEG NPs and 25 to 66% for PLGA-PLURONIC NPs in 30 min to 4h respectively. The effect was also similar in the L1210 cells (Fig.6.10) and the highest uptake of all the three types of NPs was seen at 100 $\mu\text{g/ml}$ concentration (45% for PLGA NP, 55% for PLGA-MPEG NP and 58% for PLGA-PLURONIC NP).

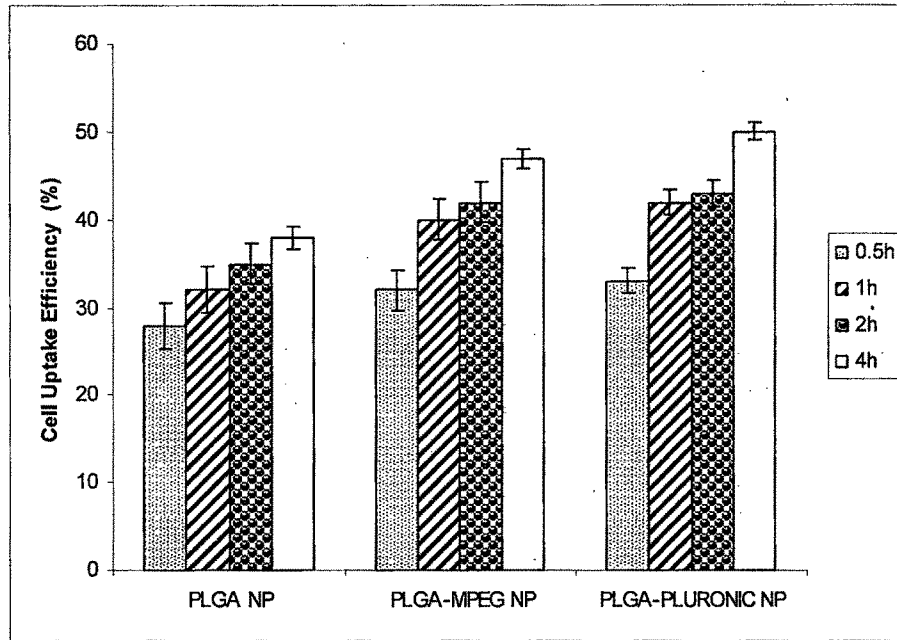


Fig. 6.7: DU145 Cell uptake efficiency (%) of PLGA, PLGA-MPEG and PLGA-PLURONIC NP at different time of 0.5, 1, 2 and 4 h at NP concentration = 100 µg/ml. Data represent mean±SD, n = 6.

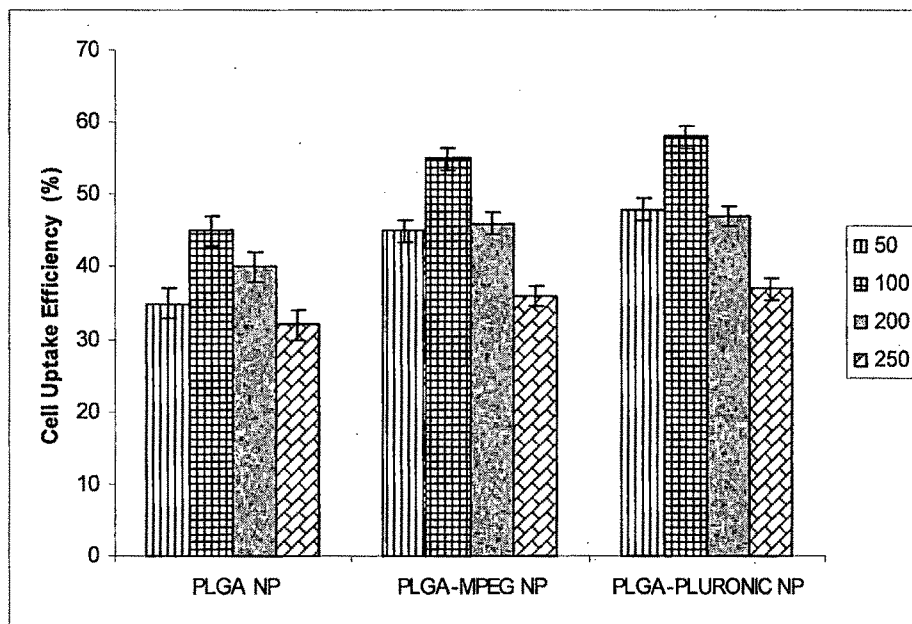


Fig. 6.8: DU145 Cell uptake efficiency (%) of PLGA, PLGA-MPEG and PLGA-PLURONIC NP at different NP Concentration of 50, 100, 200 and 250 µg/ml. Incubation time is 4h. Data represent mean±SD, n = 6.

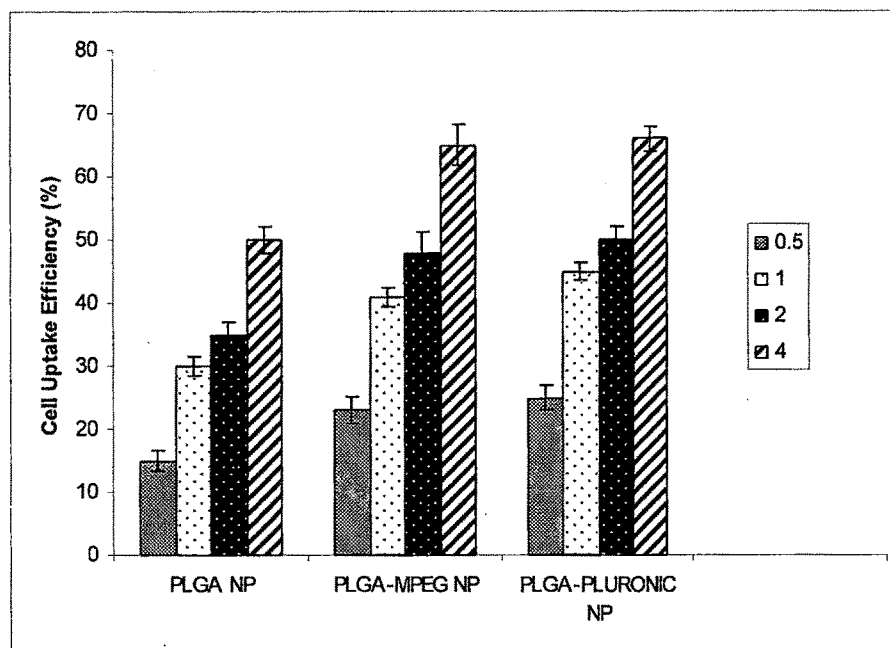


Fig. 6.9: L1210 Cell uptake efficiency (%) of PLGA, PLGA-MPEG and PLGA-PLURONIC NP at different time of 0.5, 1, 2 and 4 h at NP concentration = 100 µg/ml. Data represent mean±SD, n = 6.

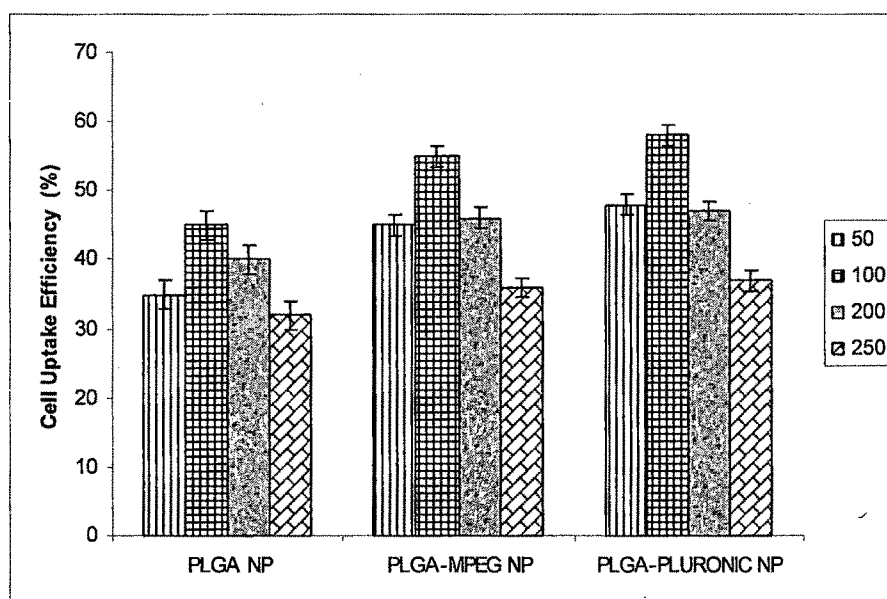


Fig. 6.10: L1210 Cell uptake efficiency (%) of PLGA, PLGA-MPEG and PLGA-PLURONIC NP at different NP Concentration of 50, 100, 200 and 250 µg/ml. Incubation time is 4h. Data represent mean±SD, n = 6.

6.13.2 Confocal microscopy

Confocal microscopy of the cells exposed to PLGA nanoparticles showed fluorescence activity in the cells within 30 min which increased with time for both the cell lines L1210 (Fig 6.11) and DU145 (Fig. 6.12). The control experiment performed by incubating cells with 6-coumarin solution (Fig. 6.11c and 6.12A) showed that intracellular fluorescence was insignificant compared to that of cells incubated with nanoparticles. Hence, it can be concluded that the fluorescence observed inside the cells was only due to the presence of nanoparticles.

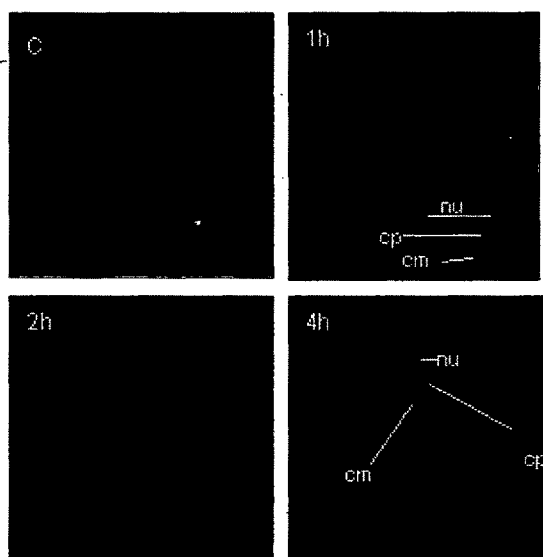


Fig. 6.11: Confocal microscope image showing cellular uptake of coumarin loaded PLGA NP at different time interval on L1210 cell lines at 37°C at 63 X oil immersion magnification. (C) is the control, (1h) image taken at 1h, the NP have been uptaken inside the cell and are inside both the cytoplasm and in nucleus, (2h) image taken after 2h, NP are seen in both cytoplasm and nucleus, intensity of fluorescence is increased (4h) image taken after 4h, the NP are seen especially in nucleus alone and very few particles are seen in cytoplasm, fluorescence intensity is maximum indicating maximum uptake.

The outline of DU145 cell is clearly seen in Fig. 6.12, in which the cell membrane (cm), cytoplasm (cp) and nucleus (nu) are seen distinctively as indicated by the arrows. At 1h, (Fig. 6.12B) the NPs are seen particularly inside the cytoplasm of the cells. In the 2h (Fig.6.12C) the NPs are seen migrating towards the nucleus and are visible in both cytoplasm and nucleus. At 4h (Fig. 6.12D), the NPs are prominently seen in the nucleus where as only a small fraction of NPs are seen in the cytoplasm.

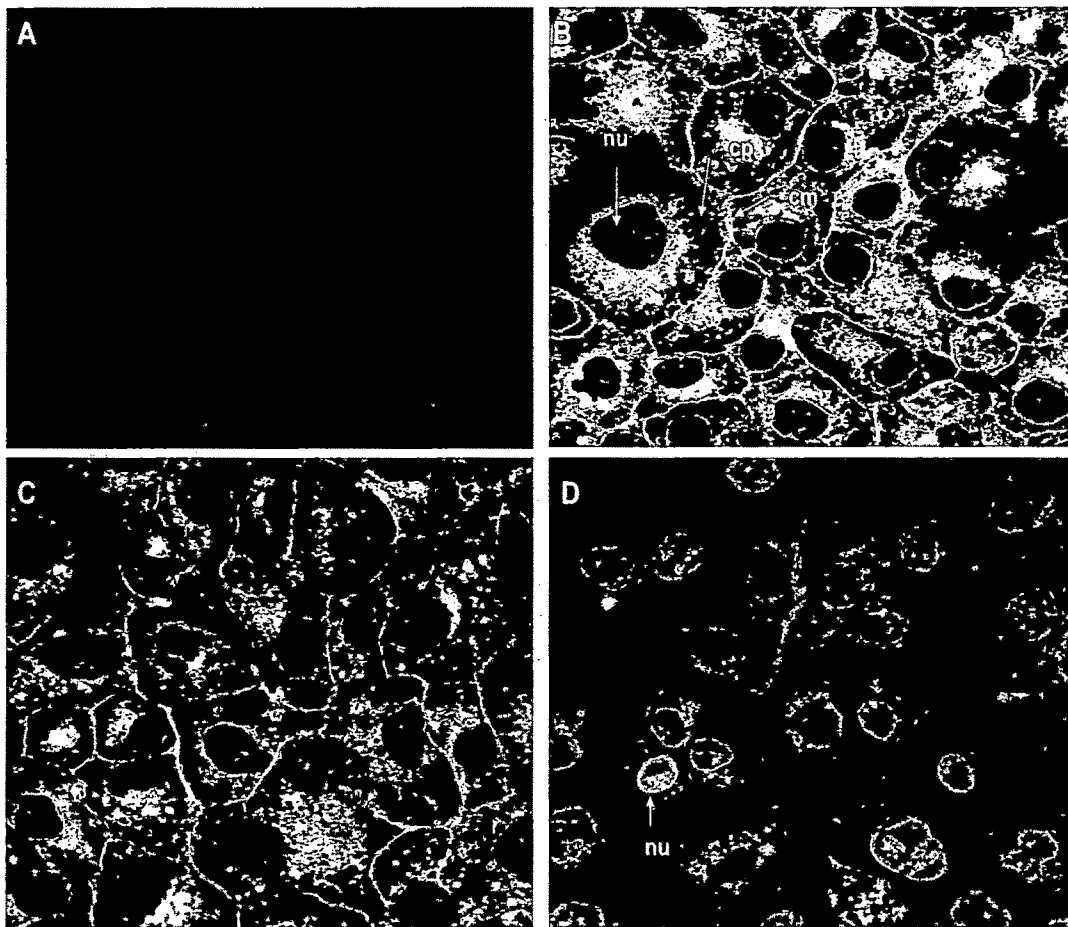


Fig. 6.12: Confocal microscope image showing cellular uptake of coumarin loaded PLGA NP at different time interval on DU145 cell lines at 37°C at 63 X oil immersion magnification. (A) is the control, (B) image taken at 1h, the NP have been uptaken inside the cell and are inside the cytoplasam, no NP seen in nucleus, (C) image taken after 2h, NP are seen in both cytoplasm and nucleus, (D) image taken after 4h, the NP are seen especially in nucleus alone and very few particles are seen in cytoplasm.

Fig 6.13 shows Z-stack Confocal images of PLGA NP showing uptake in DU 145 cells. Serial z-sections of the cells were taken and each section demonstrated fluorescence activity in between 15.1 μm and 72.3 μm from the surface of the cells (Fig 6.13) indicating that the nanoparticles were internalized by the cells and not simply bound to their surface.

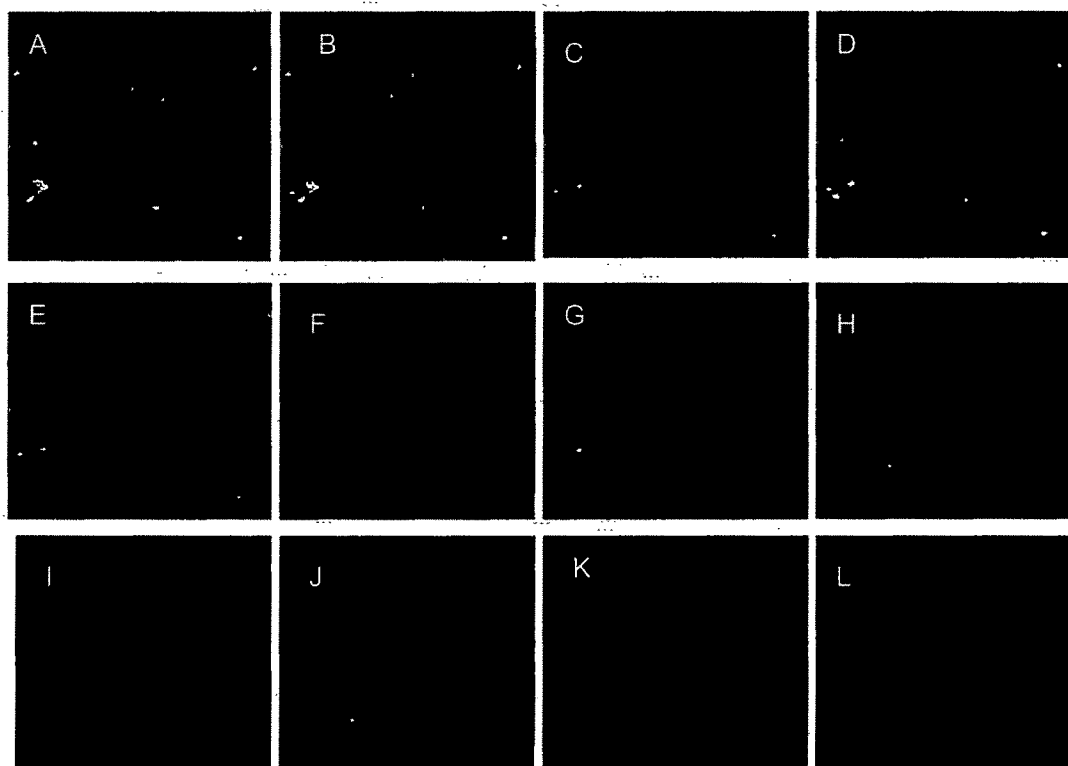


Fig. 6.13: Z stack confocal microscopy images of PLGA NP showing uptake in DU 145 cells. A= 72.3 μm , B= 68.1 μm , C=65.3 μm , D= 61.0 μm , E= 58.1 μm , F= 54.3 μm , G= 50.1 μm , H= 45.3 μm , I= 32.1 μm , J= 28.2 μm , K= 21.6 μm , L= 15.1 μm .

Fig 6.14 shows Z-stack Confocal images of PLGA-MPEG NP showing uptake in DU 145 cells. Serial z-sections of the cells were taken and each section demonstrated fluorescence activity in between 44.3 μm and 69.3 μm from the surface of the cells indicating that the nanoparticles were internalized by the DU145 cells and not simply bound to their surface.

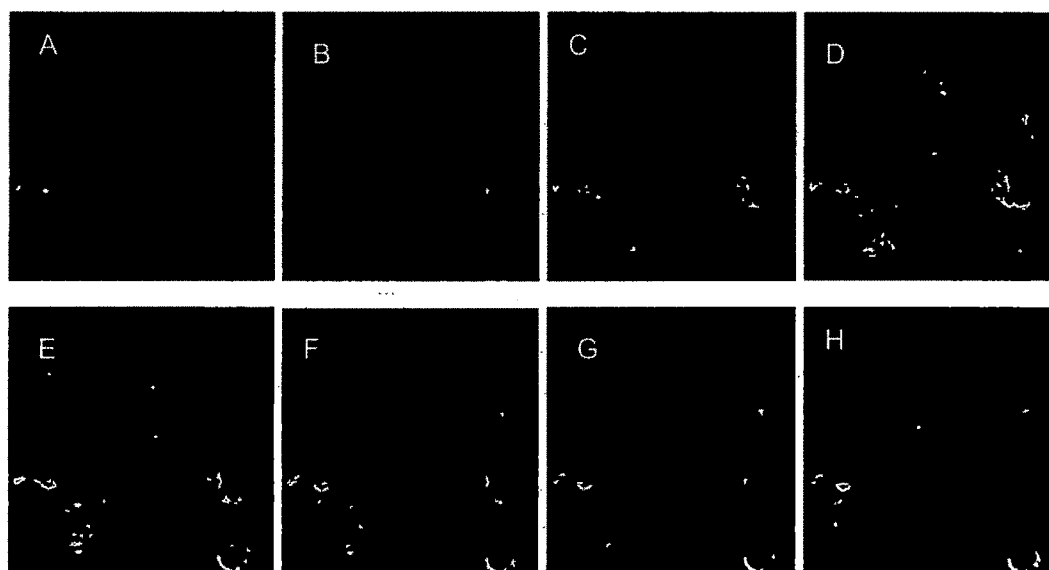


Fig. 6.14: Z stack Confocal microscopy images of PLGA-mPEG NP showing uptake in DU 145 cells. A= 53.3 μm , B= 62.1 μm , C=67.3 μm , D= 69.3 μm , E= 63.1 μm , F= 54.3 μm , G= 51.1 μm , H= 44.3 μm .

Fig 6.15 shows Z-stack Confocal images of PLGA-PLURONIC NPs showing uptake in DU 145 cells. Serial z-sections of the cells were taken and each section demonstrated fluorescence activity in between 12.8 μm and 68.4 μm from the surface of the cells, indicating that the nanoparticles were internalized by the DU145 cells and not simply bound to their surface.

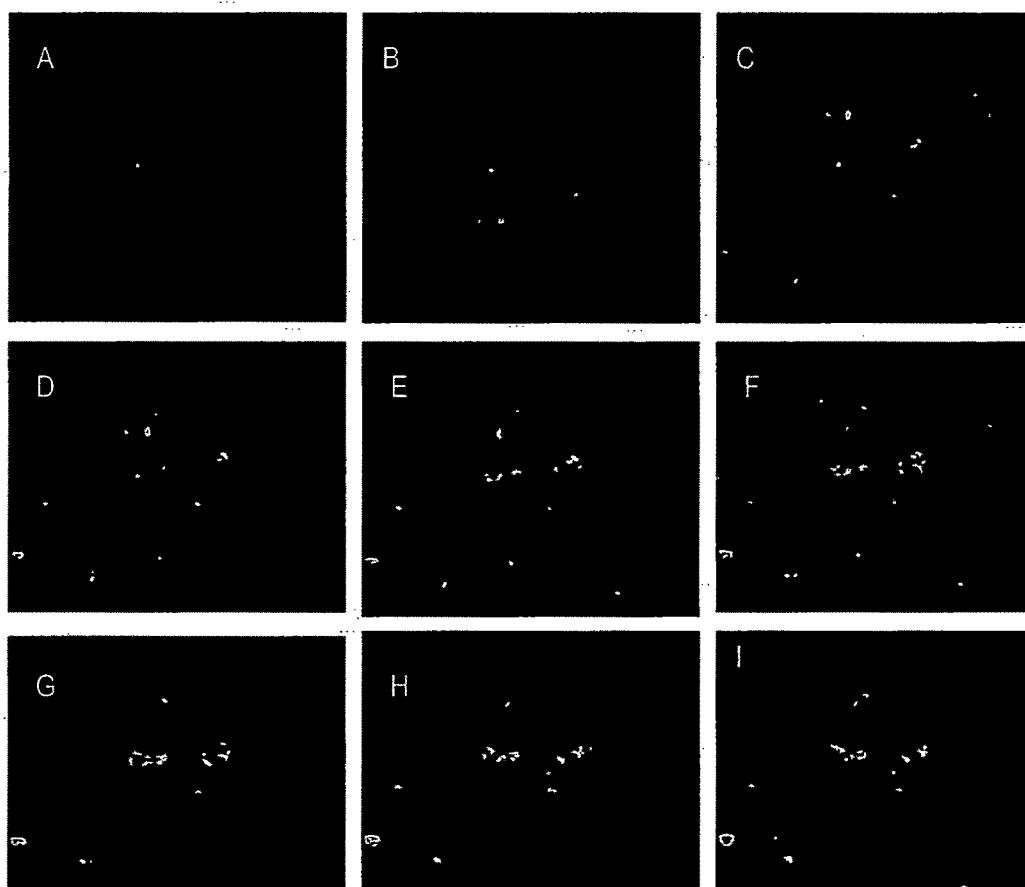


Fig. 6.15: Z stack confocal microscopy images of PLGA-Pluronic NP showing uptake in DU 145 cells. A= 12.8 μm , B= 24.1 μm , C=28.3 μm , D= 32.6 μm , E= 48.1 μm , F= 52.1 μm , G= 55.1 μm , H= 65.3 μm , I= 68.4 μm .

Fig 6.16 shows Z-stack Confocal images of PLGA-PLURONIC NPs showing uptake in L1210 cells. Serial z-sections of the cells were taken and each section demonstrated fluorescence activity in between 12.3 μm and 33.1 μm from the surface of the cells, indicating that the nanoparticles were internalized by the L1210 cells and not simply bound to their surface.

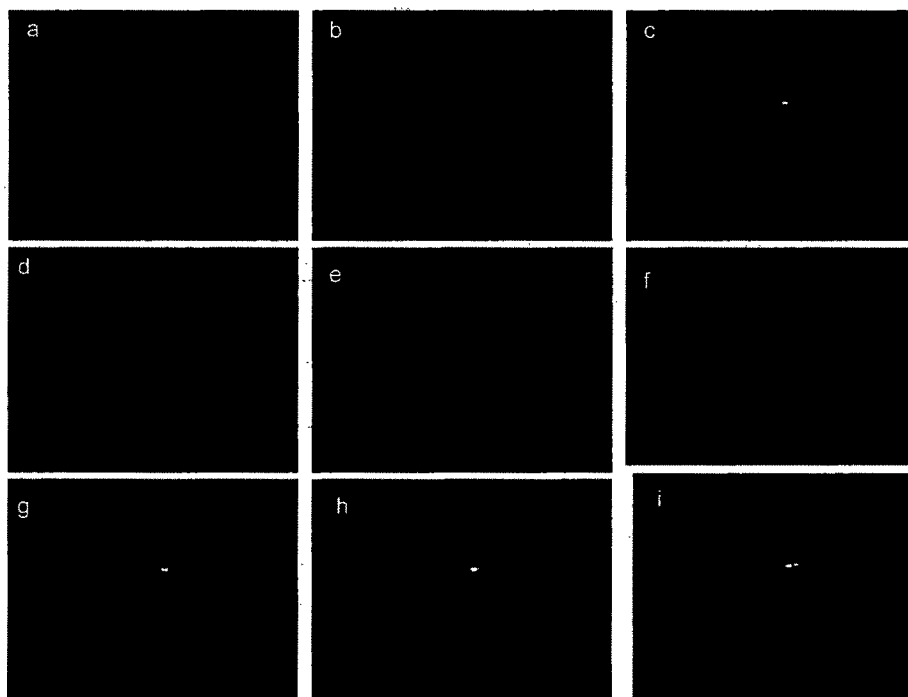


Fig. 6.16: Z stack confocal microscopy images of PLGA-PLURONIC NP showing uptake in L1210 cells. a= 12.3 μm , b= 14.2 μm , c= 16.0 μm , d= 17.0 μm , e= 18.1 μm , f= 22.3 μm , g= 26.1 μm , h= 31.4 μm , i= 33.1 μm .

Fig. 6.17 shows Z stack confocal microscopy images of PLGA-mPEG NP showing uptake in L1210 cells. A total of 16 sections were taken ranging from 5.2 μm (image 6.11p) to 75.3 μm (image 6.11h) from the surface of the cells, indicating that the nanoparticles were internalized by the L1210 cells and not simply bound to their surface.

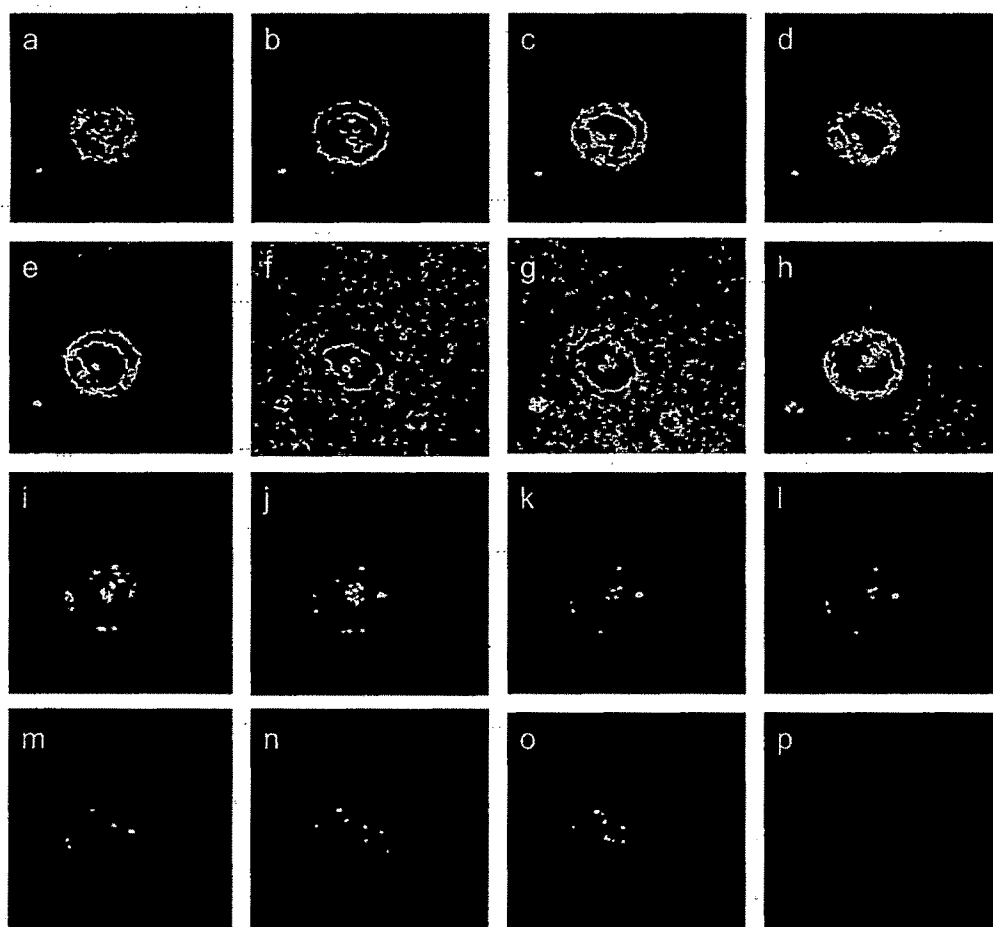


Fig. 6.17: Z stack confocal microscopy images of PLGA-mPEG NP showing uptake in L1210 cells. a= 62.3 μm , b= 64.2 μm , c= 61.0 μm , d= 57.0 μm , e= 68.1 μm , f= 68.3 μm , g= 72.1 μm , h= 75.3 μm , i= 58.1 μm , j= 48.2 μm , k= 36.6 μm , l= 25.1 μm , m= 12.8 μm , n= 10.5 μm , o= 9.2 μm , p= 5.2 μm .

Fig. 6.18 shows a comparison of Fluorescence image (F), Differential image (D) and overlap of Fluorescence Difference image (F-D) in L1210 cells for uptake of PLGA-mPEG NP. The Fluorescence images of L1210 cells does not show the clear outline of the cells and differential image gives a clear picture of the cell, but does not show the fluorescent NP. Therefore overlap of Fluorescence and Differential image (F-D) was used to give a clear picture both the cell and the fluorescent NPs. Images 1, 2 and 3 were taken at 62.3 μm and Images 4, 5 and 6 at 48.2 μm .

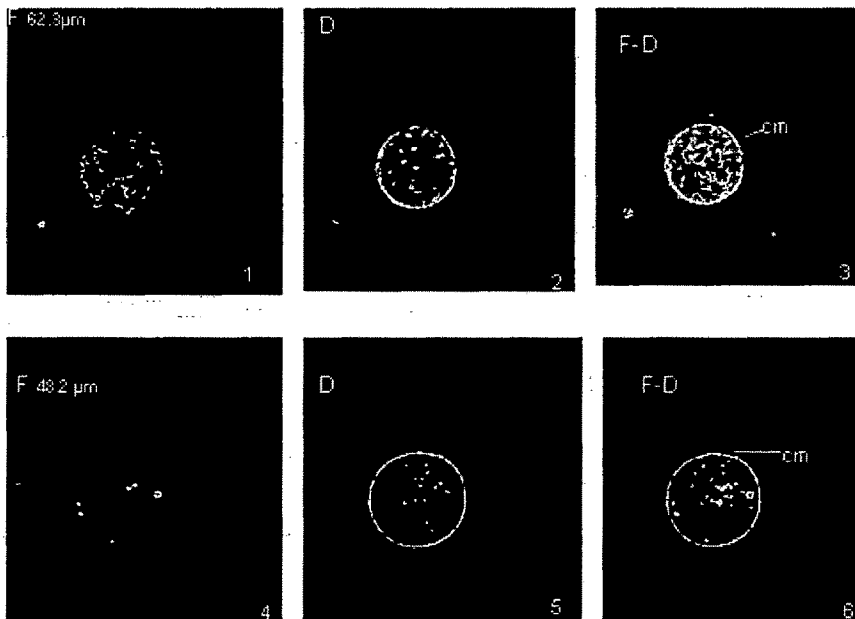


Fig. 6.18: Comparison of Fluorescence image (F), Differential image (D) and overlap of Fluorescence Difference image (F-D) in L1210 cells for uptake of PLGA-mPEG NP. The images 1,2&3 were taken at 62.3 μm and 4,5&6 at 48.2 μm .

The Fluorescence Differential images F-D3 and F-D6 show that the NPs were clearly within the L1210 cells and not merely adsorbed onto the cell.

6.13.3 Flow Cytometry

Flow cytometry study was carried out on the L1210 cell lines using 6-coumarin as the fluorescent marker in the NPs. For each cell sample, 10000 events were collected using the high-speed mode (200-300 cells/s). M1 was marked as the population of cells having fluorescence under control and M2 was marked as the population of cells with fluorescence intensity after the uptake of the NPs. Incubation of the L1210 cells with NPs caused substantial accumulation of cells in the M2 phase. Quantitative analysis of the events distribution revealed that only 16.81% of the cells were in the M2 phase for control cells (Fig. 6.19a), whereas the M2 population was increased to 42.80%, 47.81 and 51.60% for the PLGA-NP, PLGA-MPEG NP and PLGA-PLURONIC NP treated cell samples, respectively (Fig. 6.19b, c and d). These data suggest that the three formulations were effective in increasing the cell population in the M2 phase, indicating cellular uptake of the NPs.

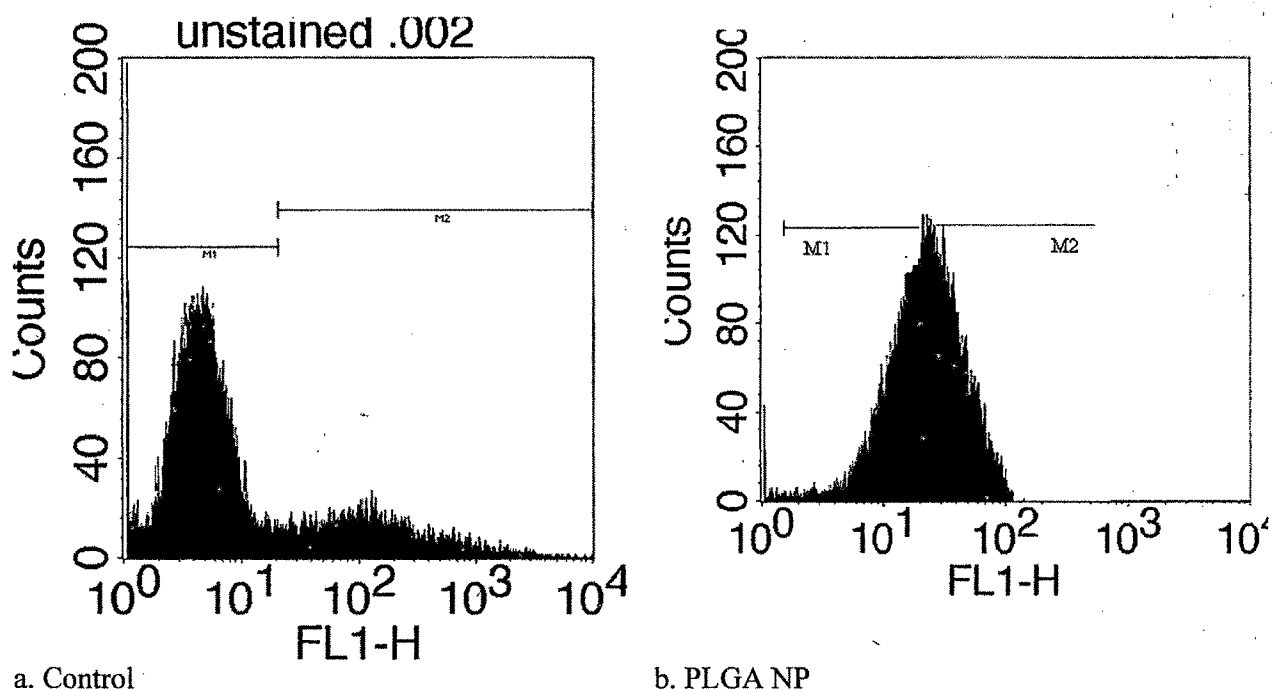


Fig. 6.19a: Flow cytometric scan of L1210 cell lines using (a)Control and (b)PLGA NPs at 37°C. M1 marks the population of cells having fluorescence under control, M2 marks the population of cells with fluorescence intensity after uptake.

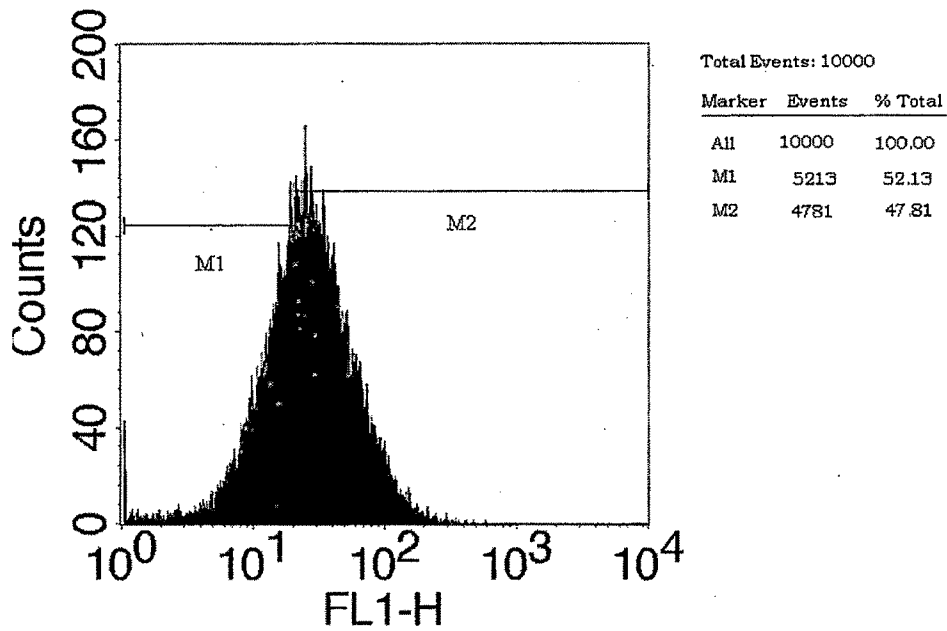


Figure 6.19c: Flow cytometric scan of L1210 cell lines using PLGA-MPEG NPs at 37°C. M1 marks the population of cells having fluorescence under control, M2 marks the population of cells with fluorescence intensity after uptake.

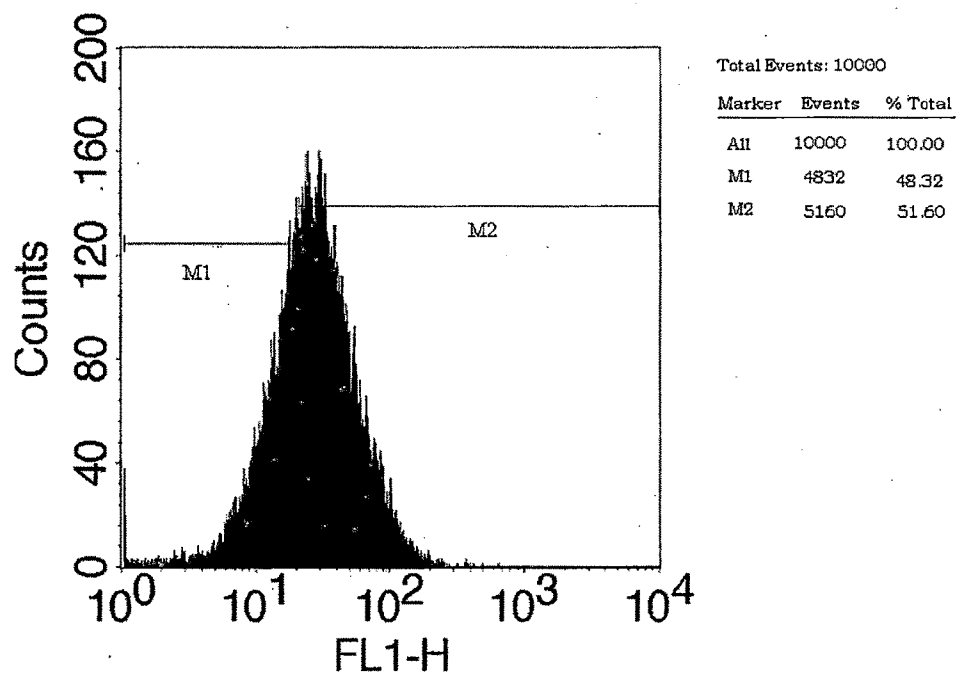


Figure 6.19d: Flow cytometric scan of L1210 cell lines using PLGA-PLURONIC NPs at 37°C. M1 marks the population of cells having fluorescence under control, M2 marks the population of cells with fluorescence intensity after uptake.

Similarly in the DU145 cells, 10000 events were collected and M1 was marked as the population of cells having fluorescence under control and M2 was marked as the population of cells with fluorescence intensity after uptake. Quantitative analysis of the events distribution revealed that incubation of the DU145 cells with NPs caused substantial accumulation of cells in the M2 phase. Quantitative analysis of the events distribution revealed that only 11.21% of the cells were in the M2 phase for control cells, M2 population was increased to 28.80%, 42.23 and 40.01% for the PLGA-NP, PLGA-MPEG NP and PLGA-PLURONIC NP treated cell samples, respectively (Fig. 6.20). These data suggest that the three formulations were effective in increasing the cell population in the M2 phase, indicating uptake of the NPs.

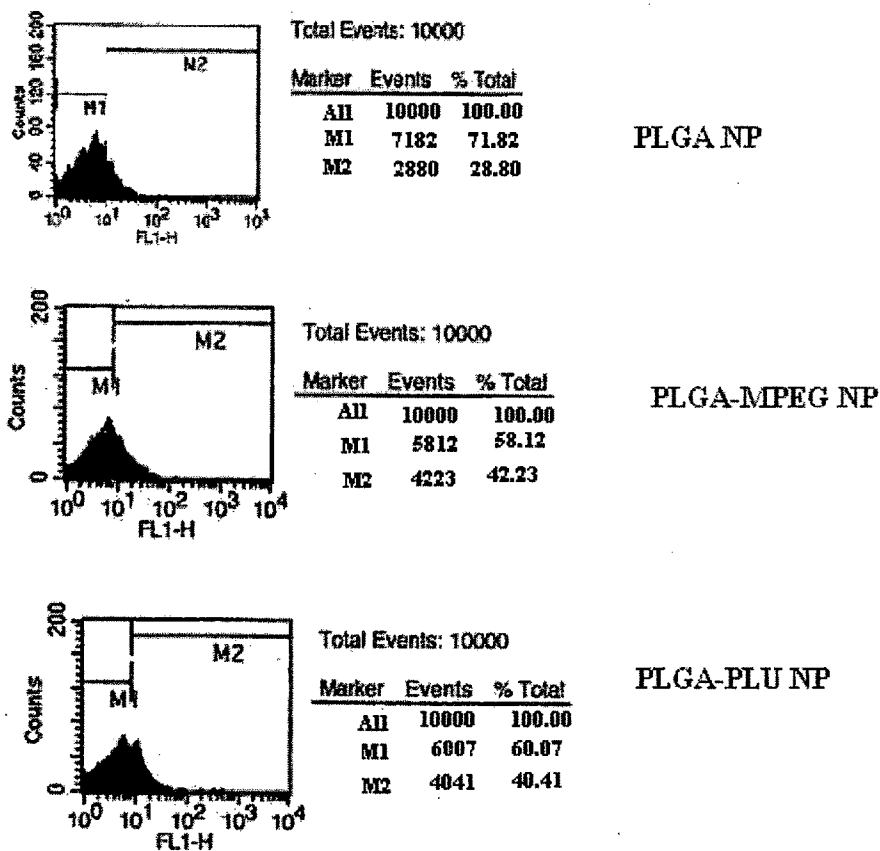


Fig. 6.20: Flow cytometric scan of DU145 cell lines using PLGA NP, PLGA-MPEG NP and PLGA-PLU NP at 37°C. M1 marks the population of cells having fluorescence under control, M2 marks the population of cells with fluorescence intensity after uptake.

REFERENCES

- Cole SP (1986). Rapid chemosensitivity testing of human lung tumor cells using the MTT assay. *Cancer Chemotherapy and Pharmacology* 17, 259–63.
- de Campos AM, Diebold Y, Carvalho ELS, Sanchez A, Alonso MJ (2004). Chitosan nanoparticles as new ocular drug delivery systems: in vitro stability, in vivo fate, and cellular toxicity. *Pharmaceutical Research* 21, 803–810.
- Dong YC, Feng SS (2004). Methoxy poly(ethylene glycol)-poly(lactide) (MPEG-PLA) nanoparticles for controlled delivery of anticancer drugs. *Biomaterials* 25, 2843–9.
- Freshney RI (1994). Measurement of viability and cytotoxicity, *Culture of Animal Cells*, 3rd Edition, Wiley-Liss, New York, 287–307.
- Lin R, Ng LS, Wang C (2005). In vitro study of anticancer drug doxorubicin in PLGA-based microparticles. *Biomaterials* 26, 4476–4485.
- Mosmann T (1983). Rapid colorimetric assay for cellular growth and survival: application to proliferation and cytotoxicity assays. *J Immunol Methods* 65, 55–63.
- Patlolla RR and Venkateswarlu V (2008). Folate-targeted etoposide-encapsulated lipid nanospheres. *Journal of Drug Targeting* 16, 269–275.
- Panyam J, and Labhasetwar V (2004). Sustained Cytoplasmic Delivery of Drugs with Intracellular Receptors Using Biodegradable Nanoparticles, *Molecular Pharmaceutics* 1, 77–84.
- Pawley JB (1995). *Handbook of Biological Confocal Microscopy*, Plenum Press, New York.
- Ramge P, Unger RE, Oltrogge JB (2000). Polysorbate-80 coating enhances uptake of polybutylcyanoacrylate (PBCA)- nanoparticles by human and bovine primary brain capillary endothelial cells. *European Journal of Neurosciences* 12, 1931–1940.
- Shim J, Kang HS, Park WS, Han SH, Kim J, Chang IS (2004). Transdermal delivery of minoxidil with block copolymer nanoparticles. *Journal of Controlled Release* 97, 477–484.
- Wartlick H, Michaelis K, Balthasar S, Strebhardt K, Kreuter J, Langer K (2004). Highly specific HER2-mediated cellular uptake of antibody-modified nanoparticles in tumour cells. *Journal of Drug Targeting* 12, 461–471.
- Win KY, Feng SS (2005). Effects of particle size and surface coating on cellular uptake of polymeric nanoparticles for oral delivery of anticancer drugs. *Biomaterials* 26, 2713–22.

Yoo HS, and Park TG (2004). Folate-receptor-targeted delivery of doxorubicin nano-aggregates stabilized by doxorubicin-PEG-folate conjugate. *Journal of Controlled Release* 100, 247-256.

Young RJ and Lovell PA (1991). Introduction to polymers. 2nd ed. London: Chapman & Hall.

Zhang Z and Feng SS (2006). The drug encapsulation efficiency, in vitro drug release, cellular uptake and cytotoxicity of paclitaxel-loaded poly(lactide)-tocopheryl polyethylene glycol succinate nanoparticles. *Biomaterials* 27, 4025-4033.